https://doi.org/10.5194/wcd-2022-50
Preprint. Discussion started: 2 September 2022

Weather and Climate Dynamics Discussions
Open Access
EGU

Anomalous subtropical zonal winds drive decreases in southern Australian frontal rain

Acacia S. Pepler[1], Irina Rudeva[1]

[1]Australian Bureau of Meteorology, Melbourne, Australia

Correspondence to: Acacia Pepler (acacia.pepler@bom.gov.au)

Abstract. Cold fronts make a significant contribution to cool season rainfall in the extratropics and subtropics. In many regions of the Southern Hemisphere the amount of frontal rainfall has declined in recent decades, but there has been no change in frontal frequency. We show that for southeast Australia this contradiction cannot be explained by changes in frontal intensity or moisture at the latitudes of interest. Rather, declining frontal rainfall in southeast Australia is associated with weakening of the subtropical westerlies in the mid troposphere, which is part of a hemispheric pattern of wind anomalies that modifies the extratropical zonal wave 3. Fronts that generate rainfall are associated with strong westerlies that penetrate well into the subtropics, and the observed decrease in frontal rainfall in southern Australia can be linked to a decrease in the frequency of fronts with strong westerlies at 25°S.

1 Introduction

Fronts are a major cause of rainfall and extremes in the global extratropics (Catto et al., 2012; Catto & Pfahl, 2013; Utsumi et al., 2017). While a large part of frontal precipitation is related to fronts embedded within extratropical cyclones (Dowdy and Catto, 2017), trailing cold fronts that are outside of the cyclone centre are an important cause of rainfall in many areas of the southern hemisphere midlatitudes and subtropics, particularly during the cool half of the year (Pepler et al., 2020; Utsumi et al., 2017).

In recent decades cool season frontal rainfall has decreased over parts of the southern hemisphere continents, including southwestern Australia (Risbey et al., 2013a), southeastern Australia (Pepler et al., 2021; Risbey et al., 2013b) and southern Africa (Burls et al., 2019). However, these studies typically found that this decrease in rainfall was not due to changes in the frequency of fronts. Indeed, studies have consistently observed little change in frontal frequency over the Southern Hemisphere midlatitudes in reanalyses (Berry et al., 2011; Rudeva & Simmonds, 2015; Solman & Orlanski, 2014), although some decreases have been observed in the frequency of midlatitude cyclones (Pepler et al., 2021; Pepler, 2020b). Frontal frequency in southeastern Australia has had little change over this period, despite expectations of a southward shift in fronts due to observed trends towards a positive Southern Annular mode (SAM) phase (Fogt & Marshall, 2020) and an intensification of the Southern Hemisphere storm track during winter (Chemke et al. 2022). Climate projections further

https://doi.org/10.5194/wcd-2022-50
Preprint. Discussion started: 2 September 2022

suggest a possible future increase in front frequency in southern hemisphere midlatitude regions (Blázquez & Solman, 2019; Catto et al., 2014), although in the subtropics frontal rainfall may still decline (Utsumi et al., 2016).

The observed decrease in frontal rainfall, in the absence of changes in frequency, suggests a change in either the moisture availability or the dynamics (e.g., intensity) of fronts that decreases the likelihood that they produce precipitation. Burls et al. (2019) investigated this for South Africa and suggested that the decrease in frontal rainfall was related to increasing atmospheric pressure in the subtropics and Hadley cell expansion. Consistent with that, Sousa et al. (2018) showed a poleward migration of 'water corridors' due to an expansion of the semi-permanent South Atlantic high-pressure system followed by a displacement of the jet-stream during the latest drought in South Africa in 2015-2017. But the extent to which these results are transferrable to elsewhere in the southern hemisphere or to longer time periods is unclear.

Southeastern Australia (SEA) is an important agricultural region of Australia, as well as home to a large proportion of Australia's population. This region has experienced significant drying since the start of the Millennium Drought (1997 – 2009), particularly during the cool season May – October, which has been linked to an intensifying subtropical ridge and anthropogenic global warming (Timbal and Drosdowsky, 2013; Rauniyar and Power, 2020). Since the end of the Millennium Drought, the annual rainfall has recovered (Fu et al., 2021); however, cool season rainfall remains below pre-drought values (Bureau of Meteorology and CSIRO, 2020; DELWP, 2020). While much of the decline in rainfall arises from decreases in both the frequency and intensity of rainfall from cyclones, there is an as-yet unexplained decline in the proportion of trailing cold fronts that produce rainfall (Pepler et al., 2021; Risbey et al., 2013b). In this study, we use front-centred composites to investigate the causes of declining frontal rainfall in southeastern Australia and the extent to which this can be linked to changes in frontal characteristics as well as large-scale circulation.

2 Data and methods

There are a large number of front identification methods, and front climatologies can be very sensitive to both the method chosen and the reanalysis product used (Soster and Parfitt, 2022; Schemm et al., 2015). While methods based on identifying a change in air mass via gradients of temperature or humidity are the most widely used, these can produce very high frequencies near coastlines (Thomas and Schultz, 2019; Schemm et al., 2015; Soster and Parfitt, 2022; Berry et al., 2011). They are also more sensitive to choices of reanalysis dataset and grid resolution than more complex front methods that also incorporate wind information (Soster and Parfitt, 2022). While front methods that incorporate both wind and temperature information have shown improved skill at representing fronts (Bitsa et al., 2021; Biard and Kunkel, 2019), for southern Australia a front detection method based solely on wind changes has shown good skill at detecting trailing cold fronts compared to manual fronts and particularly at detecting fronts associated with rainfall, with the majority of such fronts able to be confirmed by a temperature-based method (Hope et al., 2014; Pepler et al., 2020).

https://doi.org/10.5194/wcd-2022-50
Preprint. Discussion started: 2 September 2022

The wind-based front detection method is described in Rudeva & Simmonds (2015) and Simmonds et al. (2012). It compares two consecutive 6-hourly analyses of 10 m wind, and identifies a front when the horizontal wind shifts in direction from the northwest to southwest quadrant and the meridional wind increases by at least 2 m s^{-1} over 6 h. Objective features are then identified, with the easternmost edge of the frontal region for the period t to t+6h identified as a front at time t, noting that some studies suggest this may better approximate atmospheric fields at time t+6h (Papritz et al., 2014). This method is most useful for detecting cold fronts, which are the main fronts of relevance to rainfall in southern Australia. While tracking is performed for the whole southern hemisphere, this study focusses on any front that has at least two points (i.e., is at least 1° long), of which at least one is in southeast Australia (30-40°S, 135-150°E). Some supplemental analysis is also performed on fronts in southwestern Western Australia (SWWA; 23-38°S, 110-120°E), as this region is also experiencing a decline in cool season frontal rainfall (Hope et al., 2006).

All data in this paper is obtained from the ERA5 reanalysis (Hersbach et al., 2020), with fronts identified every 6 hours on a 1° grid, noting that the largest uncertainties in front frequency are found when fronts are identified on the native grid of high resolution reanalyses (Soster and Parfitt, 2022). In addition to assessing the raw front tracks, we also create front-centred composites of ERA5 data including mean sea level pressure (MSLP), rain rate, total column water (TCW), geopotential height (Z), horizontal (u, v) and vertical (w) velocity, relative vorticity, 500-1000 hPa vertically integrated moisture flux including its zonal and meridional components (IVT; Reid et al., 2022), temperature (T), divergence, static stability, and the Phillips Criterion (PC), a measure of baroclinicity. PC was calculated as in Fahad et al. (2020):

$$PC = \frac{f^2(u_{500}-u_{lower})\Theta}{\beta g H(\theta_{500}-\theta_{850})}, \quad \text{(Eq. 1)}$$

where H is the geometric height of the column—from the lower level (the average between 850 and 1000 hPa) to 500 hPa, and Θ is the reference potential temperature (300 K). While most of these variables are calculated instantaneously at the time of the front, we calculated the average rain rate from all hourly data between time t and t+6h; this can also be multiplied by 6 to represent the accumulated frontal rainfall over the corresponding period.

In some cases multiple fronts were identified in SEA at a single time, which could represent either two distinct fronts or a single system incorrectly broken into multiple parts by the tracking algorithm. To avoid double-counting any dates in composites, we created a single "merged front" for each timestep over the latitudes 20-50°S, which was used to extract front-centred data within 10° of longitude from the front location at each latitude for plotting and analysis. The merged front data was created using a four-step process, summarised in Figure 1:

1. Identify all fronts that touch the region of interest (30-40°S, 135-150°E) at a given time.
2. If there is more than one front, first identify whether they overlap at any latitudes. If they do, iteratively remove the fronts with the smallest length within the region until there is only one front identified at each latitude. Where

https://doi.org/10.5194/wcd-2022-50
Preprint. Discussion started: 2 September 2022

Weather and Climate Dynamics Discussions
Open Access
EGU

multiple overlapping fronts have the same length, we prioritise retaining fronts that are nearer in longitude to the front with the most points in the region.

3. If there are still multiple fronts, check for cases where there is 3° or less of longitude difference between the neighbouring ends of the two fronts. If so, merge them into one front and set all missing points to the average of the longitudes at the end of each segment. Otherwise, remove the event with fewest points
4. Set the central longitude of points north or south of the last front point to be equal to the last point.

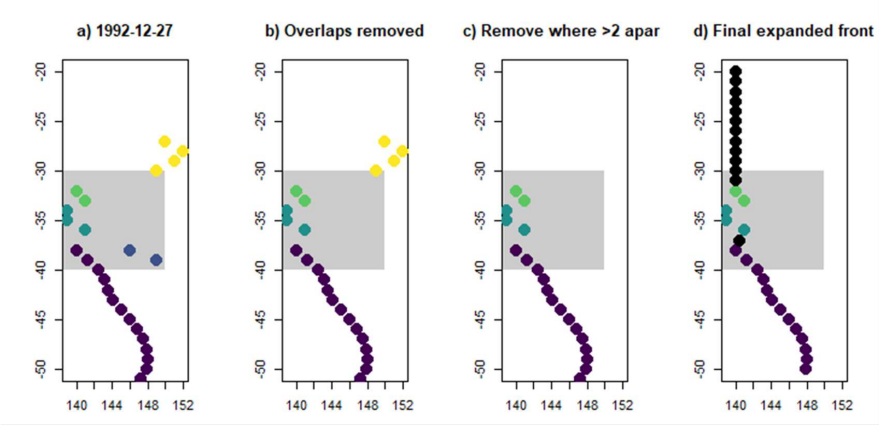

Figure 1. a) An example of the front merger process for 0000UTC on 1992-12-27, with colours indicating the five distinct fronts identified at this time and a grey box indicating the SEA tracking domain. b) Of two overlapping fronts, the one with the largest number of points in the SEA region is retained, and the other is removed. c) A front at the far north of the region is removed, as it is too far east of the other identified front points. d) At latitudes with no identified front point, the longitude is inferred based on the closest frontal points (black dots).

Results are presented for the cool season May-October, with the twenty-year periods 1980-1999 and 2000-2019 compared and statistical significance calculated using a Student's t-test. We additionally use three periods, 1979-1996, 1997-2009 and 2010-2019 in some instances to test for recovery in frontal rainfall following the Millennium drought. Unless otherwise specified, front-centred averages are calculated within +-5° of the front central longitude, representing the region with the majority of frontal rainfall, with a focus on southeast Australian latitudes 33-38°S. As the anomalous trends in rainfall are in particular a feature of trailing fronts (Pepler et al., 2021), we used a dataset of Australian cyclones detected using ERA5 (Pepler, 2020a) to compare changes in trailing fronts with those for fronts embedded in extratropical cyclones. Noting that in earlier studies the area of cyclone rainfall is often taken as 10-12° around the cyclone centre (Hawcroft et al., 2012; Pepler et al., 2020), we considered a front to be embedded in a cyclone if a cyclone centre was detected within the 135-150°E, 20-45°S region (Hawcroft et al., 2012; Pepler et al., 2020), or a trailing front if there was no cyclone in this region. During May-

https://doi.org/10.5194/wcd-2022-50
Preprint. Discussion started: 2 September 2022

October, 70% of detected fronts are considered trailing fronts, as are 55% of fronts with rain rates exceeding 0.1 mm/h in southeast Australia, as rain rates are higher in cases where cyclone and front areas overlap (Dowdy & Catto, 2017; Pepler et al., 2020).

Pearson's correlation coefficients are calculated using linearly detrended data to assess relationships between seasonal mean frontal characteristics and the intensity and position of the subtropical ridge calculated over 140-150°E (Timbal and Drosdowsky, 2013) as well as the Troup (1965) Southern Oscillation Index (SOI; http://www.bom.gov.au/climate/enso/soi/), an indicator of the El Niño-Southern Oscillation (ENSO), and the Dipole Mode Index, an indicator of the Indian Ocean Dipole (IOD: Saji et al., 1999; https://stateoftheocean.osmc.noaa.gov/sur/ind/dmi.php). Statistical significance is assessed using a Student's t-test for $p<0.05$; this is calculated using seasonal mean data for differences between periods, and between all fronts when identifying significant differences in structure between the wet and dry subsets.

3 Changes in frontal rainfall

We first assess changes in front statistics using the raw ERA5 output over 1979-2019. There is a front detected somewhere in southeast Australia at approximately 50% of time steps during May-October, with no significant difference in frequencies between the Millennium drought in 1997-2009 (49%) and the non-drought periods (50.6%). No change in front frequency is found when comparing the periods 1980-1999 and 2000-2019 for southeast Australia as a whole, or for the frequency of fronts detected for each latitude band within this region (Figure 2b). There is also no change in the average front intensity at these latitudes, defined as the strength of the change in meridional winds. There is a weak decrease in front frequency at the equatorward edge of the region influenced by fronts (20-25°S), from 22.3% to 21.5% of hours per year, but this is not statistically significant.

Figure 2a shows the average rain rate for hours with an identified front in southeast Australia, centred on the longitude of the front. Rain rates greater than 0.1 mm/h are recorded within 5 degrees of longitude on either side of the front location, with heaviest rain rates slightly west of the front line. We thus define frontal rainfall to be the average over a 10° region centred on the frontal line (0°), and use the 0° line to separate rainfall into "prefrontal" and "postfrontal" rainfall. The likelihood of frontal rainfall and the average annual frontal rainfall are highest south of 37°S. While the frequency of detected fronts remains higher than 100/season as far north as 25°S, the average rainfall from fronts decreases rapidly north of 33°S, suggesting that the northern edge of fronts is typically too weak or dry to produce rainfall.

https://doi.org/10.5194/wcd-2022-50
Preprint. Discussion started: 2 September 2022

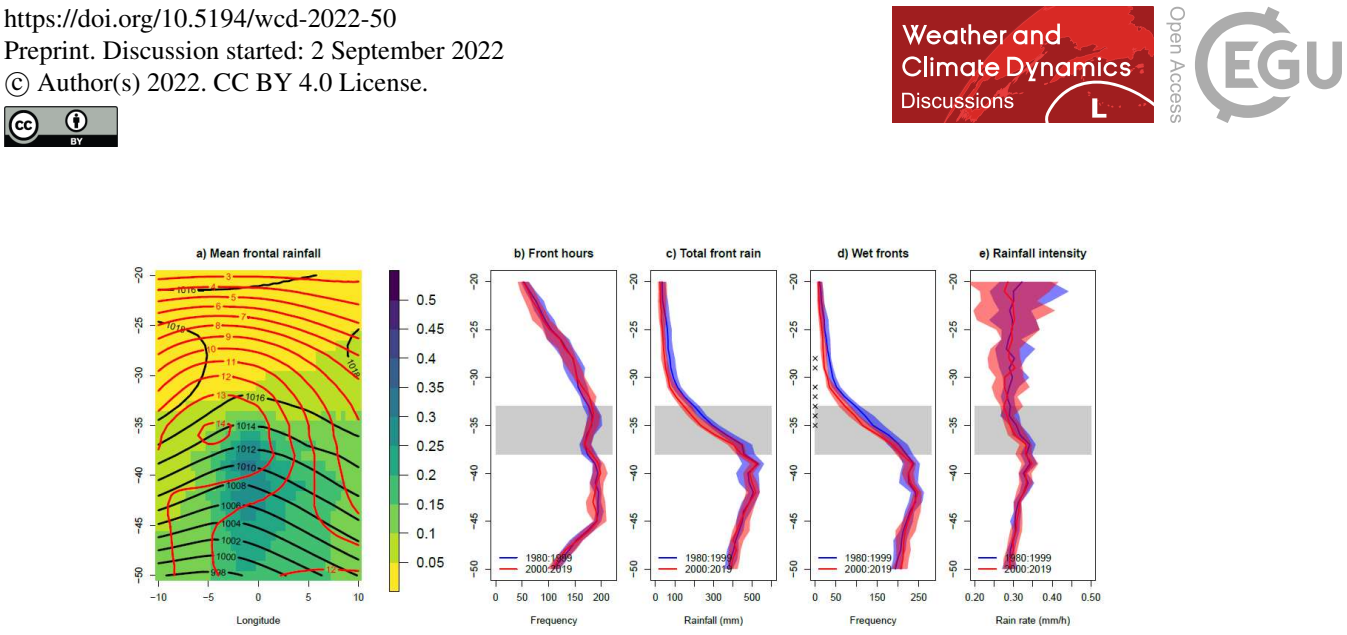

Figure 2. a) Average rain rate (shading, mm/h), MSLP (black contours) and 700 hPa zonal wind (red contours) for all hours with at least one front in SEA during May to October, centred on the longitude of the front. b) Average number of timesteps in May-October with at least one front identified at each latitude within the longitudes 135-150°E, based on the full dataset of southern hemisphere fronts prior to the merging process. Blue and red lines show the median for 1980-1999 and 2000-2019, respectively, while shading shows the interquartile range from seasonal data. c-e) Total accumulated frontal rainfall (c), number of fronts with rainfall > 0.1 mm/h (d) and average rain rate where rain is >0.1 mm/h (e) across all May-October timesteps with a front detected in SEA using the merged front dataset in 1980-1999 and 2000-2019. In b-e, crosses indicate the differences are statistically significant at p<0.05.

Comparing the periods 1980-1999 and 2000-2019, total May-October frontal rainfall has declined at all latitudes north of 38°S (Figure 2c). In SEA (33-38°S) there has been a statistically significant decrease in the mean rain rate across all front days, from 0.155 mm/h to 0.138 mm/h (-11%). This accumulates to a 32mm (9.4%) decline in total frontal rainfall in these latitudes between the two periods, with larger relative declines in rainfall further north where average frontal rainfall is smaller. This decline is not related to any change in front frequency (Figure 2b) but due to a decrease in the average rainfall intensity calculated across all fronts. This decrease in intensity is due to a decrease in the likelihood that a front will produce measurable rain in these latitudes (Figure 2d) and a corresponding increase in dry fronts, consistent with Pepler et al. (2021); for fronts that produce rainfall, the average rainfall intensity has not changed (Figure 2e).

The number of fronts per season with rainrates exceeding 0.1 mm/h in SEA decreased from 164 to 140 between 1979-1996 and 1997-2009 (-14%, p=0.01), with little recovery over the recent period 2010-2019 (145 per season). There is a decrease in the likelihood that a front will produce rainfall whether or not the front is collocated with a cyclone. The total accumulated rainfall in the prefrontal region (0 to +5°) declines by 14%, which is larger than the rainfall decline in the postfrontal region (-5%). This is in contrast to Burls et al. (2019), who found that the largest decline in south African rainfall occurred on postfrontal days.

https://doi.org/10.5194/wcd-2022-50
Preprint. Discussion started: 2 September 2022

Weather and Climate Dynamics Discussions
Open Access
EGU

4 Comparison of wet and dry fronts

Given the observed decrease in the proportion of fronts that generate rainfall, we now investigate how the characteristics of wet and dry fronts differ during 1980-1999. We define a front as being wet if the average rainrate over 33-38°S and within ±5° of the frontal line is at least 0.1 mm/h, which is satisfied by 51% of May-October fronts in 1980-1999.

Wet and dry fronts differ in many aspects (Figure 3a-f). They have more negative (stronger) vertical velocities at all levels, with the largest differences in the mid troposphere (500-700hPa); stronger cross-front gradients in temperature as well as meridional wind (not shown); and stronger relative vorticity, particularly behind the front. These variables all indicate that rain-bearing fronts are stronger in southeast Australia than those that produce little rain. Total column water and integrated vapour transport (not shown) are also higher for rain-bearing fronts at SEA latitudes as well as to the north, noting that the moisture for rain events in southeastern Australia is generally sourced from the oceans to the south (Holgate et al., 2020). Rain-bearing fronts show a higher pre-frontal Phillips Criterion, a measure of baroclinicity, to the north of 35°S, and lower prefrontal baroclinicity further south. This decrease in the Phillips Criterion to the south may be explained by consumption of baroclinity during rainfall, which leads to even stronger reduction in PC after the front. On the other hand, higher PC in rain-bearing fronts to the north of 35°S promotes stronger moisture uplift.

While there is only a small difference in mean zonal winds at the latitudes of interest, in fronts that produce rainfall there are stronger westerlies north of 33°S but weaker zonal winds south of 38°S (Figure 1f). This reflects a change in the mean patterns of winds at all levels, with the strongest relationships between rainfall and zonal winds found at 700hPa. For instance, the latitude where 700hPa zonal winds are strongest during wet fronts is 34.9°S, 6° further north than for dry fronts (40.9°S). This means that wet fronts have strong 700hPa zonal winds (defined as $u > 10$ m/s) reaching 25.4°S on average, and average zonal wind speeds of 10.8 m/s at 23-27°S. In contrast, strong westerlies only reach 30.6°S for dry fronts, and wind speeds near 25°S are half as strong (4.7 m/s). There is also a smaller but statistically significant difference in the northernmost latitude where any front is identified in the longitudes 135-150°E, which is 26.5°S for fronts with rainfall and 27.9°S for dry fronts.

https://doi.org/10.5194/wcd-2022-50
Preprint. Discussion started: 2 September 2022

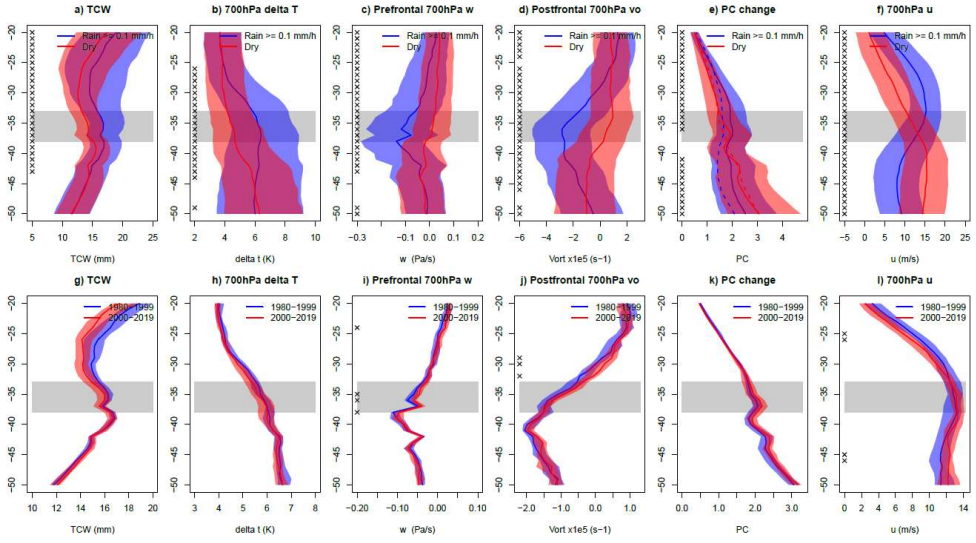

Figure 3. (a-f) Mean (line) and interquartile range (shading) of 6 variables at each latitude for May-October fronts in 1980-1999 with rain rates of at least 0.1 mm/h at 33-38°S compared to dry fronts: a) Total column water (±5° of front); b) Difference between maximum and minimum 700hPa temperature (±10° of front), indicating strength of the temperature change; c) Prefrontal 700 hPa vertical velocity (0° to +5°); d) Postfrontal (-5 to 0°) 700hPa relative vorticity; e) Mean prefrontal Phillips Criterion (0 to +5°), a measure of baroclinity, with dashed lines showing the postfrontal medians (-10° to -5° behind front); f) 700hPa zonal wind (±5° of front); (g-l) As in top row, but for the median and interquartile range of the seasonal mean value across all fronts in 2000-2019 vs 1980-1999. Crosses indicate where the two sets are statistically significantly different for p<0.05 at that latitude.

5 Changes in frontal characteristics

Having identified key aspects of fronts that differ between wet and dry fronts, we now investigate how these have changed between 1980-1999 and 2000-2019, to help identify any changes in frontal mean characteristics that decrease the likelihood of frontal rainfall.

Comparing the average across all fronts in 1980-1999 with fronts in 2000-2019 (Figure 3g-l), there has been a very small decline (-1.3%) in the average TCW at 33-38°S on front days, suggesting moisture availability is unlikely to be a major contributor to changes in frontal rainfall. Changes in metrics of front intensity at these latitudes such as the average change in meridional wind speed or change in temperature across the frontline are also very small (<3%). There is no statistically significant change in baroclinicity measured by the Phillips Criterion in southeast Australian latitudes, although there is a reduction to the south. There is a statistically significant decrease (-14%) in the prefrontal 700hPa vertical velocity in SEA, coinciding with the longitudes of the largest rainfall decline (Figure 2c, i), and a weak, non-significant increase in postfrontal vertical velocity. There is also a statistically significant weakening of post-frontal relative vorticity over 33-38°S (-11%),

https://doi.org/10.5194/wcd-2022-50
Preprint. Discussion started: 2 September 2022

Weather and Climate Dynamics Discussions
Open Access
EGU

with larger changes in vorticity to the north. While these changes are generally weak, and not necessarily aligned with the latitudes most relevant to our region of interest, together they are suggestive of an overall weakening of frontal baroclinicity. There are larger changes in both moisture variables and indicators of frontal intensity between the two periods at latitudes north of 30°S, including mean meridional wind change (not shown), relative vorticity, and mean zonal winds. This indicates a weakening of the northward edge of the front and a southward shift of frontal features. Between 1980-1999 and 2000-2019 there has been no change in the average northernmost latitude with a detected front. However, the mean northernmost latitude of zonal winds exceeding 10 m/s has shifted from 28.0°S to 28.8°S, associated with a 12% decline in the mean zonal wind speed at 23-27°S, noting that these two variables are strongly correlated (r=+0.74).

To assess the extent to which various front characteristics can be tied to changes in frontal rainfall we apply multiple linear regressions between frontal rainfall and one or more explanatory factors over 1980-1999. We then apply the regression coefficients to the 2000-2019 period to calculate the reduction in mean rainfall expected from observed changes in the predictors, and divide this by the observed rainfall change between the two periods to calculate the proportion of rainfall change explained by those factors. We found that a single linear regression between mean zonal winds at 23-27°S and mean frontal rainfall at 33-38°S over 1980-1999 is able to explain 59% of the decrease in average frontal rainfall. The proportion of rainfall decline explained can be increased by adding either prefrontal vertical velocity (71%) or TCW (81%); as TCW and w are correlated (-0.42), there is no additional predictive value from a three-variable regression. Predictive skill is similar but slightly lower if we use the northernmost latitude of zonal winds exceeding 10 m/s combined with TCW (71%). In contrast, single linear regressions with either vertical velocity (32%) or TCW (25%) explain only a small proportion of the rainfall change.

These multiple linear regressions typically underestimate the higher end of frontal rainfall, as the relationship between frontal rainfall and both zonal winds and TCW are nonlinear. Fronts with strong westerlies extending to at least 23°S have average rain rates over 33-38°S more than three times higher than fronts where strong westerlies are only observed up to 30°S. During 1980-1999, only 27% of fronts had westerlies extending to 23°S, but these fronts explained 42% of all frontal rainfall over SEA.

Between 1979-1996 and 1997-2009, i.e., before and during the Millennium Drought, there was a 28% decrease in the frequency of fronts with 700hPa westerlies extending north of 23°S, and a 34% (54 mm, p=0.01) decrease in their accumulated rainfall over SEA (Figure 4). There has been little recovery following the Millennium drought, with frequencies in 2010-2019 25% below the 1979-1996 average and rainfall 25% below the 1979-1996 average. As there is no overall change in the frequency of fronts during or after the drought, the decrease in the number of fronts with westerlies north of 23°S is balanced by an increase in the frequency of fronts where westerlies are poleward of 23°S, and a corresponding weak increase in associated rainfall (+8 to +13mm). The decrease in the frequency of fronts where westerlies extend northward of

https://doi.org/10.5194/wcd-2022-50
Preprint. Discussion started: 2 September 2022

Weather and Climate Dynamics Discussions
Open Access
EGU

255 23°S is thus sufficient to explain the entirety of the observed change in frontal rainfall at 33-38°S during the period since 1997.

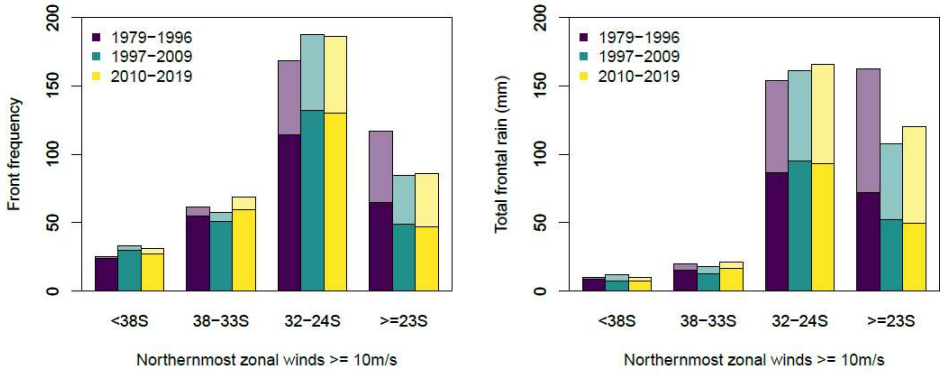

260 **Figure 4. The average frequency (left) and total accumulated rainfall in 33-38°S (right) for May-October fronts in 1979-1996, 1997-2009 and 2010-2019, separated by the northernmost latitude where 700hPa zonal winds exceed 10 m/s. Each bar shows the total across all fronts, with darker shading indicating the component from trailing fronts and lighter shading showing the component from fronts embedded in a cyclone.**

To test the role of cyclones in this result, we further separated our analysis between trailing fronts and fronts associated with 265 a cyclone. Almost half (44%) of fronts with westerly winds extending north of 23°S had an associated low, which is higher than the frequency of lows across all fronts (29%). When comparing 1979-1996 and 1997-2009, there was a 27% decline ($p=0.03$) in rainfall from trailing fronts and a larger 39% decline ($p=0.008$) in rainfall from fronts that *co-occurred* with a cyclone, indicating that declines in frontal rainfall can in part be linked to the observed decrease in the frequency of low pressure systems in this period (Pepler et al. 2021), as any change in low pressure systems will also affect rainfall from 270 embedded fronts . In comparison, the 2010-2019 period has seen a partial recovery of rainfall from embedded fronts (22% below the 1979-1996 average), but no recovery in rain from trailing fronts (-31%). This may indicate the change in rainfall from trailing fronts is playing an increasingly large role in overall rainfall declines, although differences between 1997-2009 and 2010-2019 are not statistically significant. Meanwhile, for fronts where strong westerly winds are south of 23°S, both those with and without cyclones have increased in frequency, indicating that the westerly winds are playing a stronger role in 275 rainfall changes than interactions with cyclones.

https://doi.org/10.5194/wcd-2022-50
Preprint. Discussion started: 2 September 2022

Weather and Climate Dynamics Discussions
Open Access
EGU

6 Links to large-scale circulation

While we have demonstrated that declines in rainfall at 33-38°S can be explained by a weakening and southward shift of the northern edge of the front, this raises a subsequent question: given that we have shown no decrease in the frequency or intensity of fronts such as their 700hPa longitudinal temperature gradient, measures of frontal baroclinicity such as the Phillips criterion, or even the latitude of fronts as identified using a wind-based front identification scheme, what is the driver of this weakening? We propose that this is related to changes in the atmopheric extratropical circulation in the SH.

Between 1980-1999 and 2000-2019 there has been a change in MSLP and wind anomalies suggestive of wave number 3 (Figure 5c). The strongest anomaly in the MSLP is observed over the southern Atlantic ocean, associated with an easterly anomaly in both 700hPa and 300hPa winds around 40°S and westerly anomaly around 60°S. Weaker trends towards higher pressure and easterly wind anomalies are also evident around 100°E and 220°E, with corresponding westerly anomalies to the south. Areas of anticyclonic anomalies are interspersed with cyclonic anomalies, which are typically slightly poleward. Additional analysis of the meridional wind showed that these changes act to modify the climatological zonal wave 3 (ZW3), defined as the leading EOF of the monthly meridional wind as in Goyal et al. (2022) but using 700 hPa where we see the largest wind change in fronts (Figure A1). However, changes to the ZW3 do not represent a perfect zonal wave, possibly due to interactions with other wave numbers and local forcings, hence, no trend in either intensity or location of the climatological ZW3 was found. With the exception of very strong anomalies such as in the southern Atlantic and most northward parts of the two other anticyclonic anomalies, most of other changes in the SH circulation are not statistically significant, including in eastern Australia (Figure A2).

This hemispheric wavy pattern of anomalies is still apparent when data is separated into days with (Figure 5a) and without (Figure 5b) a front in southeast Australia. However, on front days the wave pattern is amplified and there are easterly wind anomalies at 700hPa over northeastern Australia, with weak easterly anomalies extending to 300hPa, and westerly anomalies as well as below average pressure to the south of Australia, consistent with the composites shown in Figure 3. (We note here that the low pressure anomaly to the south of Australia is located further south than the area that was considered for separation between embedded and trailing fronts). The topography of New Zealand then acts as a barrier to the intensified westerlies around 45°S, with return flow potentially contributing to the anticyclonic anomaly in the Tasman Sea and therefore the stronger subtropical easterly anomalies. This pattern of zonal wind anomalies is weaker or absent on days with no front in SEA, with increasing MSLP over the Australian Bight and westerly anomalies at 300hPa over northeast Australia. This demonstrates a more complex relationship between changes in the mean state and synoptic anomalies. An anticyclonic anomaly to the east of Australia on front days suggests Rossby wave breaking, noting that SEA is known for high number of Rossby wave breaking events (de Vries, 2021) and cut-off lows (Portmann et al., 2021).

https://doi.org/10.5194/wcd-2022-50
Preprint. Discussion started: 2 September 2022

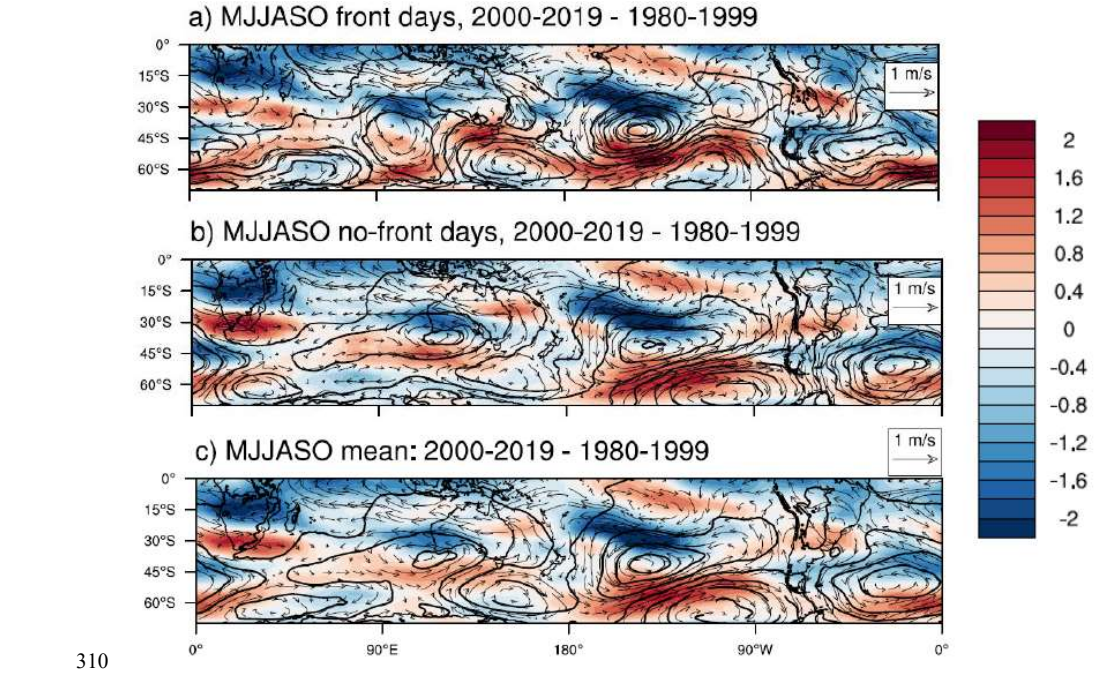

Figure 5. Anomalies of May-October 300hPa zonal wind speed (shading, every 0.2 m/s), 6-hourly mean sea level pressure (black contours, every 0.5 hPa), and 700hPa winds (vectors) between 1980-1999 and 2000-2019 in ERA5 for a) Front hours only, b) Hours without a front in southeast Australia, and c) Seasonal mean change.

To test the statistical significance of wind changes, we calculated the average zonal wind anomalies for each latitude band over eastern Australia, 135-150°E. There are no statistically significant changes in seasonal mean 300hPa winds between 1980-1999 and 2000-2019 at any latitude, with weak westerly anomalies (0.3 m/s) around 25°S, easterly anomalies (~ -0.35 m/s) around 30-35°S, and stronger westerly anomalies southward (Figure 5c). This mean pattern combines very different patterns over eastern Australia between days with and without fronts, which had trends of opposite signs over most of 20-40°S. In contrast to the mean change, there was a weak subtropical easterly anomaly on front days, averaging -0.4 m/s over 20-25°S, in agreement with an anticyclonic anomaly to the east of Australia. Subtropical anomalies are more consistent at 700hPa with a mean zonal wind change of -0.6 m/s at 20-25°S, which is stronger for front days (-0.8 m/s, p=0.08) than for no-front days (-0.4 m/s).

https://doi.org/10.5194/wcd-2022-50
Preprint. Discussion started: 2 September 2022

Weather and Climate Dynamics Discussions
Open Access
EGU

7 Drivers of interannual variability

To test the role of major climate drivers in observed changes, we calculated the detrended correlations between the annual number of fronts in May-October, as well as associated winds and rainfall with a number of climate indices over the same months (Table 1). The overall frequency of fronts is negatively correlated with the intensity and position of the subtropical ridge, with fewer fronts when the ridge is strong or shifted to the south, noting that cold fronts are typically linked to the strom tracks and westerlies and are less likely to be identified in easterly wind regimes to the north of the ridge. These correlations are a result of very strong negative correlations between both indices (STRI and STRP) and the frequency of wet fronts, with weaker positive correlations between the STR and dry fronts. The STR is also very strongly correlated with the average northernmost latitude of strong westerlies for fronts and the number of fronts with strong westerlies north of 23°S. However, it is only weakly correlated with the seasonal mean zonal winds at 20-25°S, with stronger negative correlations between STRI and zonal winds between 26-35°S. This may indicate a role of the STR in keeping frontal weserlies south and thus influencing frontal rainfall; however, the STR itself is also influenced by pressure variations associated with synoptic systems so the relationship may be more complex.

Table 1. Detrended earson's correlations between front frequency, rainfall, and the northernmost latitude with 700 hPa zonal wind >= 10 m/a (strong winds) and 6 climate indices for May-October, 1979-2019 (1982-2019 for DMI and NINO3.4). Also shown are the partial correlations for NINO3.4 and DMI. Bold indicates significance for p<0.05.

Variable	STRI	STRP	SOI	NINO3.4	DMI	SAM	NINO3.4 - DMI	DMI - NINO3.4
Front days	**-0.53**	**-0.58**	0.28	-0.19	-0.19	-0.12	-0.13	-0.09
Total front rainfall	**-0.66**	**-0.53**	**0.56**	**-0.40**	**-0.68**	0.08	-0.11	**-0.62**
Number of wet fronts	**-0.76**	**-0.65**	**0.56**	**-0.42**	**-0.60**	-0.01	-0.17	**-0.53**
Number of dry fronts	**0.34**	0.18	**-0.35**	0.28	**0.48**	-0.09	0.04	**0.45**
Average latitude of U>=10m/s	**-0.78**	**-0.65**	**0.57**	**-0.36**	**-0.67**	-0.08	-0.04	**-0.63**
Number of fronts with strong winds north of 23S	**-0.73**	**-0.60**	**0.51**	-0.30	**-0.65**	0.02	0.03	**-0.62**
Number of fronts with strong winds south of 23S	**0.38**	0.22	**-0.34**	0.17	**0.55**	-0.10	-0.13	**0.56**

https://doi.org/10.5194/wcd-2022-50
Preprint. Discussion started: 2 September 2022

There were no statistically significant correlations between the seasonal mean SAM and front frequency or rainfall, which may be a consequence of the large intraseasonal variability in SAM. There was also no correlation between fronts and NINO3.4 after accounting for covariations with DMI, with the stronger correlations with SOI potentially due to interactions between the Indian Ocean Dipole and sea level pressure at Darwin. Interestingly, however, while DMI was not strongly correlated with the seasonal frequency of fronts, it had a very strong correlation with both total frontal rainfall and the frequency of wet fronts, which was independent of any effect of ENSO. DMI also had strong correlations with the average northernmost latitude of strong frontal westerlies, consistent with the link between the IOD and the mean westerlies in southeast Australia (Pepler et al., 2014), resulting in a signifcant increase in frontal rainfall during years with a negative IOD.

These results show that wet and dry fronts can have very different relationships with climate drivers, resulting in the weaker relationships that have previously been identified between front frequency and DMI (Rudeva and Simmons 2015). Negative Indian Ocean Dipole events and a weaker subtropical ridge (negative STRI) allow front-related westerlies to extend further north, resulting in an increased frequency of wet fronts, although statistically significant correlations between these drivers and the seasonal mean zonal wind are only identified south of 26°S. Note that the DMI is correlated with both the intensity (+0.58) and position (+0.32) of the subtropical ridge during this season, so these relationships are not independent, and an equatorward shift in fronts may itself cause changes in the pressure fields which are used to calculate the STR.

During the period 1979-2019, there has been a weak increasing trend in the intensity of the sutropical ridge, of 0.26 hPa/decade (p=0.09), consistent with longer-term increases over the historical record (Timbal & Drosdowsky 2013). This may partially explain the observed trends in wet fronts: while there is a statistically significant linear trend in the number of wet fronts over 1979-2019 (-0.92 fronts/y, p=0.03), this trend becomes weaker and nonsignificant after removing variability associated with the subtropical ridge intensity (-0.35 fronts/y). Removing the subtropical ridge also had a similar effect on trends in frontal winds.

8 Changes in fronts in southwest western Australia

The very strong easterly anomalies at 700hPa and 300hPa identified over southwest Western Australia in Figure 5 raise the question of whether changes in the background zonal winds are also playing a role in rainfall declines in this region. Similar to southeast Australia, SWWA (110-120°W) has seen little decrease in the frequency of fronts between 1980-1999 and 2000-2019, but a statistically significant 11% (38mm) decrease in total frontal rainfall, particularly prefrontal rainfall (-21%), which is linked to a decrease in the frequency of rainbearing fronts (Figure A3). The average differences between wet and dry fronts are also similar between the two regions, with the most significant change relevant to frontal rainfall observed in the zonal winds to the north of SWWA (Figure A4). And, consistent with SEA, there has been a 21% decrease in the

https://doi.org/10.5194/wcd-2022-50
Preprint. Discussion started: 2 September 2022

frequency of fronts in SWWA with strong 700hPa westerlies extending north of 23°S and a 44mm (-23%) decline in associated rainfall, which explains the entirety of the observed decline in frontal rainfall. The extratropical circulation on SWWA front days resembles the zonal wave 3 pattern shown for SEA in Figure 4a, with the low pressure anomaly to the south of Australia shifted westward (Figure A5).

9 Discussion and Conclusions

Frontal rainfall is influenced by a large number of factors, including available moisture (e.g., TCW) and frontal dynamics (e.g., temperature/wind change, vertical velocity, and relative vorticity). This is consistent with other studies (Solari et al., 2022) and suggests that changes in any of these variables could result in changes in frontal rainfall. However, while the frequency of rain-bearing fronts is decreasing during the cool season in many parts of the southern hemisphere midlatitudes, including in southeast Australia, this decrease is occurring despite little change in front frequency (Burls et al., 2019; Pepler et al., 2021; Risbey et al., 2013b), as well as little change in metrics of frontal moisture or traditional measures of front intensity, beyond a slight weakening of average prefrontal vertical velocity and postfrontal vorticity.

There has been no observed change in the mean latitude of tracked fronts in southeast Australia during the cold season, consistent with previous studies (e.g., Rudeva & Simmonds 2015), despite decreases in the frequency of associated cyclones. However, if the northernmost edge of the front is instead defined as the northernmost latitude with strong westerly winds, here defined as 700hPa zonal winds >= 10 m/s, we see a 1° southward shift in the mean equatorward extent of fronts over this period. We find a particularly strong decline in the frequency of fronts with strong westerlies north of 23°S, which were responsible for 42% of frontal rainfall at 33-38°S between 1980-1999. This highlights an aspect of frontal intensity and associated rainfall that is worthy of further research, and may be relevant to other regions of the southern hemisphere. There has also been a decrease in the overall intensity of the subtropical westerlies over eastern Australia and many other areas of the southern hemisphere, consistent with Simmons (2022), although the trend in the mean state is weaker than on front days. Frontal winds and rainfall have shown little recovery since the end of the millenium drought, and may be part of a longer-term decline in cool season rainfall over this region.

Timbal & Drosdowsky (2013) identified an intensification of the subtropical ridge during the early 21st century, which they proposed as a major cause of rainfall declines in southeast Australia during the years 1997-2009. This decline has continued, with the average intensity of the May-October subtropical ridge at 140-150°E increasing by 0.26 hPa/decade over the period 1979-2019. There has also been an increase in the mean sea level pressure and a weakening of the background zonal wind speeds in subtropical Australia. We find that the northern edge of the front and the likelihood of fronts producing rainfall show strong statistical relationships with the intensity and position of the subropical ridge, suggesting a possible link between trends in pressure and frontal rainfall. A link between decreasing frontal rain and increasing pressure was also

https://doi.org/10.5194/wcd-2022-50
Preprint. Discussion started: 2 September 2022

identified by Burls et al. (2019) in southern Africa. However, the nature of this relationship depends on the location of the subtropical ridge and mechanisms may differ on frontal and non-frontal days. We also found that frontal rainfall is favoured during negative IOD conditions, consistent with Lawrence et al. (2022), and that IOD has a stronger influence on frontal rainfall than frequency. While robust trends cannot be calculated for the IOD over this short time period, paleoclimate data indicates that positive IOD events may be becoming more common (Abram et al., 2020).

An alternate explanation could be due to links between the mid-tropospheric frontal westerlies and the strength or location of the subtropical jet. In constrast to the observed strengthening of the subtropical ridge, there have been no robust trends identified in the southern hemisphere subtropical jet (Maher et al., 2019). However, a weakening of 700hPa zonal winds between 20-35°S during July was also identified for southeast and southwest Australia by Osbrough & Frederiksen (2021), which they linked to decreases in July baroclinicity and rainfall in southern Australia. Our analysis also indicates no change in the latitude of the subtropical jet (not shown), but a possible weakening in its intensity on front days in eastern Australia, although the average change in zonal wind speed is smaller at 300hPa than it is at 700hPa. The mean state changes in Figures 5 and S1 are also indicative of a modification of the ZW3 in the Southern Hemisphere , which has been associated with rainfall variability in parts of southeast Australia but has no clear trend in the cool season (Campitelli et al., 2021).

The strong link between frontal rainfall and changes in the subtropical 700hPa westerlies was tested for a second region that has experienced declines in cool season frontal rainfall, southwest Western Australia, with remarkably similar results. Easterly 300hPa wind anomalies and 850hPa moisture flux in the subtropics have also been noted during dry winters in Southern Africa (Mahlalela et al., 2019), which is another region which has experienced decreases in winter rainfall (Sousa et al., 2018; Burls et al., 2019) and weakening of the subtropical westerlies between 1980-1999 and 2000-2019. These results raise the question of what role changes in subtropical zonal winds may be playing in frontal rainfall in other areas of the southern hemisphere. Future work will develop a more generalisable approach to investigate how the northern extent of frontal westerlies is changing in other parts of the southern hemisphere, as well as how this is likely to change in the future climate given the projected poleward shift in the storm tracks and the edge of the Hadley Cell (IPCC, 2021). This may provide a potential avenue to reconcile projected changes in cool season rainfall across southern hemisphere midlatitude regions (IPCC, 2021) with the lack of change projected in frontal frequency (Catto et al., 2014).

Data availability

The merged front datasets for SEA and SWWA are available online at https://figshare.com/s/20e79f6ce9656124db6d. The front composites were developed using ERA5 data, which is freely available from the Copernicus Climate Change Service Climate Data Store at https://cds.climate.copernicus.eu/#!/search?text=ERA5&type=dataset

https://doi.org/10.5194/wcd-2022-50
Preprint. Discussion started: 2 September 2022

Weather and Climate Dynamics Discussions
Open Access
EGU

Acknowledgments

This work has been supported by the Victorian Department of Environment, Land, Water and Planning through the Victorian Water and Climate Initiative, and has used computing resources from the National Computational Infrastructure. We thank Sugata Narsey and Pandora Hope for their comments that have improved this manuscript.

References

Abram, N. J., Wright, N. M., Ellis, B., Dixon, B. C., Wurtzel, J. B., England, M. H., Ummenhofer, C. C., Philibosian, B., Cahyarini, S. Y., Yu, T. L., Shen, C. C., Cheng, H., Edwards, R. L., and Heslop, D.: Coupling of Indo-Pacific climate variability over the last millennium, Nature, 579, 385–392, https://doi.org/10.1038/s41586-020-2084-4, 2020.

Berry, G., Jakob, C., and Reeder, M.: Recent global trends in atmospheric fronts, Geophys. Res. Lett., 38, 1–6, https://doi.org/10.1029/2011GL049481, 2011.

Biard, J. C. and Kunkel, K. E.: Automated detection of weather fronts using a deep learning neural network, Adv. Stat. Climatol. Meteorol. Oceanogr., 5, 147–160, https://doi.org/10.5194/ascmo-5-147-2019, 2019.

Bitsa, E., Flocas, H. A., Kouroutzoglou, J., Galanis, G., Hatzaki, M., Latsas, G., Rudeva, I., and Simmonds, I.: A Mediterranean cold front identification scheme combining wind and thermal criteria, Int. J. Climatol., 6497–6510, https://doi.org/10.1002/joc.7208, 2021.

Blázquez, J. and Solman, S. A.: Relationship between projected changes in precipitation and fronts in the austral winter of the Southern Hemisphere from a suite of CMIP5 models, Clim. Dyn., 52, 5849–5860, https://doi.org/10.1007/s00382-018-4482-y, 2019.

Bureau of Meteorology and CSIRO: State of the Climate 2020, 2020.

Burls, N. J., Blamey, R. C., Cash, B. A., Swenson, E. T., Fahad, A. al, Bopape, M. J. M., Straus, D. M., and Reason, C. J. C.: The Cape Town "Day Zero" drought and Hadley cell expansion, npj Clim. Atmos. Sci., 2, 1–8, https://doi.org/10.1038/s41612-019-0084-6, 2019.

Campitelli, E., Díaz, L. B., and Vera, C.: Assessment of zonally symmetric and asymmetric components of the Southern Annular Mode using a novel approach, Clim. Dyn., 58, 161–178, https://doi.org/10.1007/s00382-021-05896-5, 2021.

Catto, J. L. and Pfahl, S.: The importance of fronts for extreme precipitation, J. Geophys. Res. Atmos., 118, 10791–10801, https://doi.org/10.1002/jgrd.50852, 2013.

Catto, J. L., Jakob, C., Berry, G., and Nicholls, N.: Relating global precipitation to atmospheric fronts, Geophys. Res. Lett., 39, L10805, https://doi.org/10.1029/2012GL051736, 2012.

Catto, J. L., Nicholls, N., Jakob, C., and Shelton, K. L.: Atmospheric fronts in current and future climates, Geophys. Res. Lett., 41, 7642–7650, https://doi.org/10.1002/2014GL061943, 2014.

DELWP: Victoria's water in a changing climate: Insights from the Victorian Water and Climate Initiative, 97 pp., 2020.

https://doi.org/10.5194/wcd-2022-50
Preprint. Discussion started: 2 September 2022

Dowdy, A. J. and Catto, J. L.: Extreme weather caused by concurrent cyclone, front and thunderstorm occurrences, Sci. Rep., 7, srep40359, https://doi.org/10.1038/srep40359, 2017.

Fahad, A. al, Burls, N. J., and Strasberg, Z.: How will southern hemisphere subtropical anticyclones respond to global warming? Mechanisms and seasonality in CMIP5 and CMIP6 model projections, Clim. Dyn., 55, 703–718, https://doi.org/10.1007/s00382-020-05290-7, 2020.

Fogt, R. L. and Marshall, G. J.: The Southern Annular Mode: Variability, trends, and climate impacts across the Southern Hemisphere, Wiley Interdiscip. Rev. Clim. Chang., 11, 1–24, https://doi.org/10.1002/wcc.652, 2020.

Fu, G., Chiew, F. H., Zheng, H., Robertson, D. E., Potter, N. J., Teng, J., Post, D. A., Charles, S. P., and Zhang, L.: Statistical analysis of attributions of climatic characteristics to nonstationary rainfall-streamflow relationship, J. Hydrol., 603, 127017, https://doi.org/10.1016/j.jhydrol.2021.127017, 2021.

Goyal, R., Jucker, M., Sen Gupta, A., and England, M. H.: A new zonal wave 3 index for the Southern Hemisphere, J. Clim., https://doi.org/10.1175/JCLI-D-21-0927.1, 2022.

Hawcroft, M. K., Shaffrey, L. C., Hodges, K. I., and Dacre, H. F.: How much Northern Hemisphere precipitation is associated with extratropical cyclones?, Geophys. Res. Lett., 39, L24809, https://doi.org/10.1029/2012GL053866, 2012.

Hersbach, H., Bell, B., Berrisford, P., Hirahara, S., Horányi, A., Muñoz-Sabater, J., Nicolas, J., Peubey, C., Radu, R., Schepers, D., Simmons, A., Soci, C., Abdalla, S., Abellan, X., Balsamo, G., Bechtold, P., Biavati, G., Bidlot, J., Bonavita, M., Chiara, G., Dahlgren, P., Dee, D., Diamantakis, M., Dragani, R., Flemming, J., Forbes, R., Fuentes, M., Geer, A., Haimberger, L., Healy, S., Hogan, R. J., Hólm, E., Janisková, M., Keeley, S., Laloyaux, P., Lopez, P., Lupu, C., Radnoti, G., Rosnay, P., Rozum, I., Vamborg, F., Villaume, S., and Thépaut, J.: The ERA5 Global Reanalysis, Q. J. R. Meteorol. Soc., 1–51, https://doi.org/10.1002/qj.3803, 2020.

Holgate, C. M., Evans, J. P., van Dijk, A. I. J. M., Pitman, A. J., and Di Virgilio, G.: Australian precipitation recycling and evaporative source regions, J. Clim., 1–40, https://doi.org/10.1175/jcli-d-19-0926.1, 2020.

Hope, P., Keay, K., Pook, M., Catto, J., Simmonds, I., Mills, G., McIntosh, P., Risbey, J., and Berry, G.: A Comparison of Automated Methods of Front Recognition for Climate Studies: A Case Study in Southwest Western Australia, Mon. Weather Rev., 142, 343–363, https://doi.org/10.1175/MWR-D-12-00252.1, 2014.

Hope, P. K., Drosdowsky, W., and Nicholls, N.: Shifts in the synoptic systems influencing southwest Western Australia, Clim. Dyn., 26, 751–764, https://doi.org/10.1007/s00382-006-0115-y, 2006.

IPCC: Climate Change 2021: The Physical Science Basis. Contribution of Working Group I to the Sixth Assessment Report of the Intergovernmental Panel on Climate Change, 2021.

Lawrence, L., Parfitt, R., and Ummenhofer, C. C.: The role of atmospheric fronts in austral winter precipitation changes across Australia, Atmos. Sci. Lett., 1–9, https://doi.org/10.1002/asl.1117, 2022.

Maher, P., Kelleher, M. E., Sansom, P. G., and Methven, J.: Is the subtropical jet shifting poleward?, Clim. Dyn., 54, 1741–1759, https://doi.org/10.1007/s00382-019-05084-6, 2019.

https://doi.org/10.5194/wcd-2022-50
Preprint. Discussion started: 2 September 2022

Mahlalela, P. T., Blamey, R. C., and Reason, C. J. C.: Mechanisms behind early winter rainfall variability in the
505 southwestern Cape, South Africa, Clim. Dyn., 53, 21–39, https://doi.org/10.1007/s00382-018-4571-y, 2019.

Osbrough, S. L. and Frederiksen, J. S.: Interdecadal changes in Southern Hemisphere winter explosive storms and Southern Australian rainfall, Clim. Dyn., https://doi.org/10.1007/s00382-021-05633-y, 2021.

Papritz, L., Pfahl, S., Rudeva, I., Simmonds, I., Sodemann, H., and Wernli, H.: The Role of Extratropical Cyclones and Fronts for Southern Ocean Freshwater Fluxes, J. Clim., 27, 6205–6224, https://doi.org/10.1175/JCLI-D-13-00409.1, 2014.

510 Pepler, A.: Australian region cyclones, 1950-2019, https://doi.org/https://doi.org/10.6084/m9.figshare.c.4944135.v1, 2020a.

Pepler, A.: Record Lack of Cyclones in Southern Australia During 2019, Geophys. Res. Lett., 47, https://doi.org/10.1029/2020GL088488, 2020b.

Pepler, A., Timbal, B., Rakich, C., and Coutts-Smith, A.: Indian ocean dipole overrides ENSO's influence on cool season rainfall across the Eastern seaboard of Australia, J. Clim., 27, 3816–3826, https://doi.org/10.1175/JCLI-D-13-00554.1, 2014.

515 Pepler, A. S., Dowdy, A. J., van Rensch, P., Rudeva, I., Catto, J. L., and Hope, P.: The contributions of fronts, lows and thunderstorms to southern Australian rainfall, Clim. Dyn., 55, 1489–1505, https://doi.org/10.1007/s00382-020-05338-8, 2020.

Pepler, A. S., Dowdy, A. J., and Hope, P.: The differing role of weather systems in southern Australian rainfall between 1979 – 1996 and 1997 – 2015, Clim. Dyn., 2289–2302, https://doi.org/10.1007/s00382-020-05588-6, 2021.

520 Portmann, R., Sprenger, M., and Wernli, H.: The three-dimensional life cycles of potential vorticity cutoffs: a global and selected regional climatologies in ERA-Interim (1979–2018), Weather Clim. Dyn., 2, 507–534, https://doi.org/10.5194/wcd-2-507-2021, 2021.

Rauniyar, S. P. and Power, S. B.: The impact of anthropogenic forcing and natural processes on past, present and future rainfall over Victoria, Australia, J. Clim., 33, 8087–8106, https://doi.org/10.1175/JCLI-D-19-0759.1, 2020.

525 Reid, K. J., King, A. D., Lane, T. P., and Hudson, D.: Tropical, Subtropical and Extratropical Atmospheric Rivers in the Australian Region, J. Clim., 1–26, https://doi.org/10.1175/JCLI-D-21-0606.1, 2022.

Risbey, J. S., Pook, M. J., and McIntosh, P. C.: Spatial trends in synoptic rainfall in southern Australia, Geophys. Res. Lett., 40, 3781–3785, https://doi.org/10.1002/grl.50739, 2013a.

Risbey, J. S., Mcintosh, P. C., and Pook, M. J.: Synoptic components of rainfall variability and trends in southeast Australia,
530 Int. J. Climatol., 33, 2459–2472, https://doi.org/10.1002/joc.3597, 2013b.

Rudeva, I. and Simmonds, I.: Variability and trends of global atmospheric frontal activity and links with large-scale modes of variability, J. Clim., 28, 3311–3330, https://doi.org/10.1175/JCLI-D-14-00458.1, 2015.

Saji, N. H., Goswami, B. N., Vinayachandran, P. N., and Yamagata, T.: A dipole mode in the tropical Indian Ocean, Nature, 401, 360–363, https://doi.org/10.1038/43854, 1999.

535 Schemm, S., Rudeva, I., and Simmonds, I.: Extratropical fronts in the lower troposphere–global perspectives obtained from two automated methods, Q. J. R. Meteorol. Soc., 141, 1686–1698, https://doi.org/10.1002/qj.2471, 2015.

https://doi.org/10.5194/wcd-2022-50
Preprint. Discussion started: 2 September 2022

Simmonds, I., Keay, K., and Bye, J. A. T.: Identification and climatology of Southern Hemisphere mobile fronts in a modern reanalysis, J. Clim., 25, 1945–1962, https://doi.org/10.1175/JCLI-D-11-00100.1, 2012.

Simmons, A. J.: Trends in the tropospheric general circulation from 1979 to 2022, Weather Clim. Dyn. Discuss., Preprint, 777–809, 2022.

Solari, F. I., Blázquez, J., and Solman, S. A.: Relationship between frontal systems and extreme precipitation over southern South America, Int. J. Climatol., 1–15, https://doi.org/10.1002/joc.7663, 2022.

Solman, S. A. and Orlanski, I.: Poleward Shift and Change of Frontal Activity in the Southern Hemisphere over the Last 40 Years, J. Atmos. Sci., 71, 539–552, https://doi.org/10.1175/JAS-D-13-0105.1, 2014.

Soster, F. and Parfitt, R.: On Objective Identification of Atmospheric Fronts and Frontal Precipitation in Reanalysis Datasets, J. Clim., 1–57, https://doi.org/10.1175/jcli-d-21-0596.1, 2022.

Sousa, P. M., Blamey, R. C., Reason, C. J. C., Ramos, A. M., and Trigo, R. M.: The 'Day Zero' Cape Town drought and the poleward migration of moisture corridors, Environ. Res. Lett., 13, 124025, https://doi.org/10.1088/1748-9326/aaebc7, 2018.

Thomas, C. M. and Schultz, D. M.: What are the Best Thermodynamic Quantity and Function to Define a Front in Gridded Model Output?, Bull. Am. Meteorol. Soc., 100, 873–896, https://doi.org/10.1175/bams-d-18-0137.1, 2019.

Timbal, B. and Drosdowsky, W.: The relationship between the decline of Southeastern Australian rainfall and the strengthening of the subtropical ridge, Int. J. Climatol., 33, 1021–1034, https://doi.org/10.1002/joc.3492, 2013.

Troup, A. J.: The 'southern oscillation,' Q. J. R. Meteorol. Soc., 91, 490–506, https://doi.org/10.1002/qj.49709139009, 1965.

Utsumi, N., Kim, H., Kanae, S., and Oki, T.: Which weather systems are projected to cause future changes in mean and extreme precipitation in CMIP5 simulations?, J. Geophys. Res. Atmos., 121, 2016JD024939, https://doi.org/10.1002/2016JD024939, 2016.

Utsumi, N., Kim, H., Kanae, S., and Oki, T.: Relative contributions of weather systems to mean and extreme global precipitation, J. Geophys. Res. Atmos., 122, 152–167, https://doi.org/10.1002/2016JD025222, 2017.

de Vries, A. J.: A global climatological perspective on the importance of Rossby wave breaking and intense moisture transport for extreme precipitation events, Weather Clim. Dyn., 2, 129–161, https://doi.org/10.5194/wcd-2-129-2021, 2021.

https://doi.org/10.5194/wcd-2022-50
Preprint. Discussion started: 2 September 2022

Weather and Climate Dynamics Discussions
Open Access
EGU

Appendix: Supplementary Figures

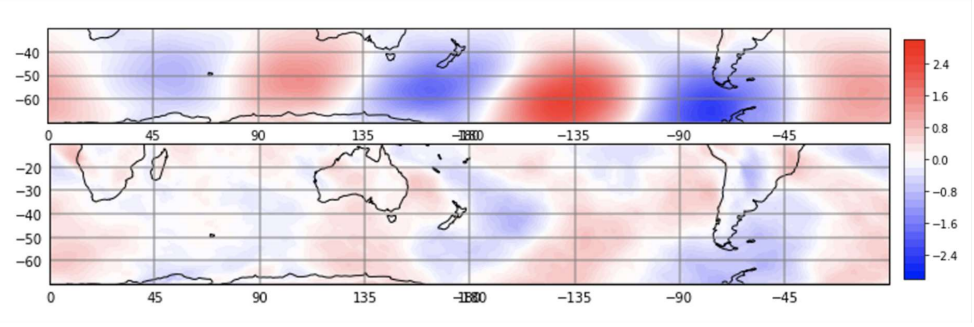

Figure A1. (top) The leading EOF of the monthly mean ERA5 meridional wind at 700 hPa during 1980-1999, scaled so that the mean Principal component equals 1; (bottom) Mean change in 700hPa meridional winds (m/s) between 1980-1999 and 2000-2019, showing that changes are offset from the climatological ZW3, particularly in the Pacific sector.

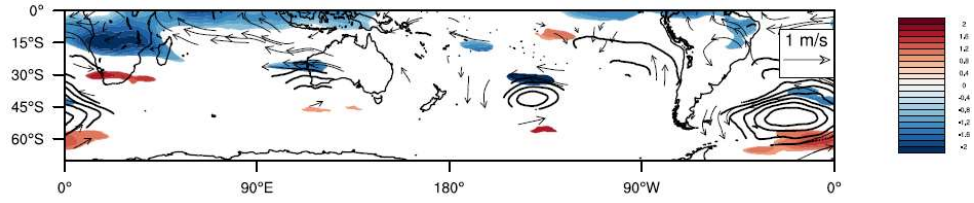

Figure A2. As in Figure 4c, but only showing trends that are statistically significant for p<0.01

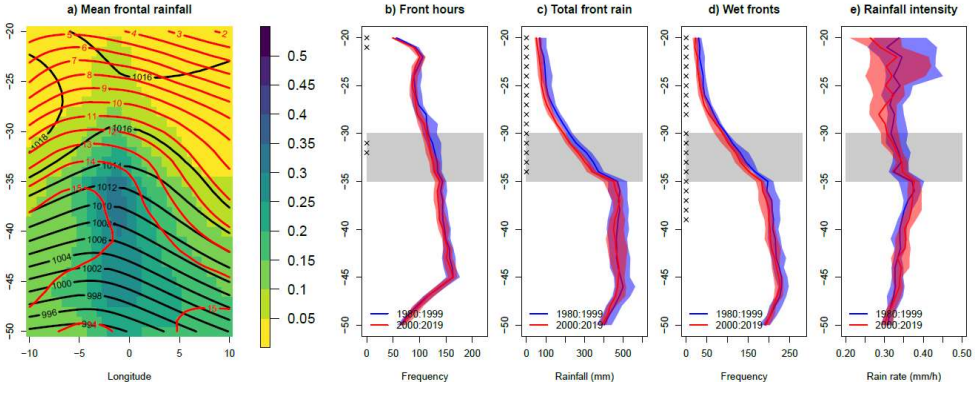

Figure A3. As in Figure 2, but for all merged fronts identified for SWWA, 110-120°E, 23-38°S

https://doi.org/10.5194/wcd-2022-50
Preprint. Discussion started: 2 September 2022

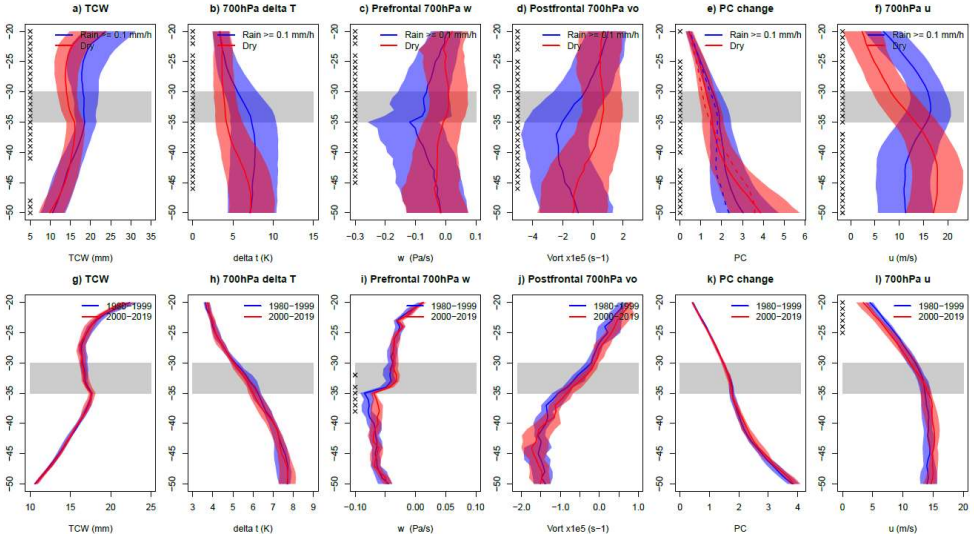

575 **Figure A4. As in Figure 3 but for fronts in SWWA: the first row separates wet and dry fronts in SWWA by mean rain exceeding 0.1 mm/h over the latitudes 30-35°S**

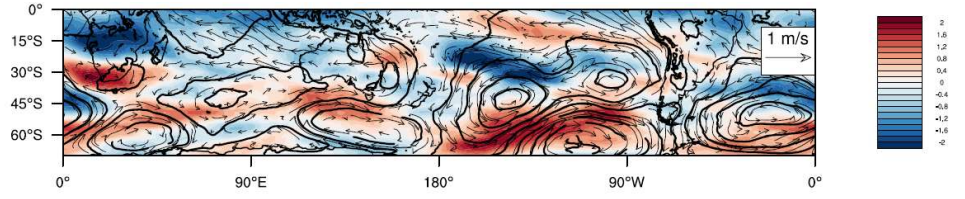

Figure A5. As in Figure 4a, but for times with a front in SWWA (110-120°E).

580